

DETECTION OF GROUNDWATER SATURATED FRACTURES USING GEOELECTRICAL TECHNIQUES OF GRADIENT PROFILING IN THE RGSC OF BANARAS HINDU UNIVERSITY, INDIA

Girija Shankar Yadav

Department of Geophysics, Faculty of Science, Varanasi, Uttar Pradesh, India

ABSTRACT

A simplified version of Gradient Profiling technique has been applied in the Rajiv Gandhi South Campus RGSC of Banaras Hindu University, Barkachha, Mirzapur district of Uttar Pradesh, India to identify the low resistive zone. The horizontal electric field was generated in the central region of widely separated two current electrodes fixed at the ground surface and the potential gradient was measured within onethird central region of the total spread using a moving dipole with considerably small electrode separation. The observations were taken along three transects. The lowest value of apparent resistivity was obtained almost in the middle portion of the fractured zone. Interested low along the profile was identified and geoelectrical sounding was also conducted at 12 such locations. One test borehole was drilled at GS8 location and groundwater discharge of about 8,000 liters per hour was obtained during the month of October 2006. Such low discharge of groundwater was obtained due to limited extent of fractures within the sandstone. The analysis presented here clearly shows the efficiency of the gradient profiling technique.

KEYWORDS: *Fractures, Gradient Profiling, Geoelectrical Sounding, Hard Rocks, Groundwater Exploration*

Article History

Received: 10 Apr 2018 / Revised: 28 Apr 2018 / Accepted: 12 May 2018

INTRODUCTION

The occurrence and movement of groundwater are governed by fractures, cracks, faults in hard rock area, and the yield depends on the size of fractures and their interconnectivity. Fractures signify concentration of void space in rocks. The geometry of the void space affects both the flow properties and the physical properties of the rock mass, such as to elastic and electric properties. An understanding, how the void space geometry controls the fluid flow and geophysical properties of the rock, forms the foundation of geophysical methods used to detect fractures in the subsurface. Geophysical methods are particularly useful for identifying large individual fractures as well as groups of closely spread and interconnected fractures or fracture zones. The low resistive zone produces high current density in the presence of horizontal electric field. There have been significant recent improvements in subsurface fracture detection techniques.

Geoelectrical methods utilize direct current (DC) so as to electric fields may satisfy the Laplace equation. In the geoelectrical methods, two electrodes are used to inject current into the ground, and two electrodes are used to measure the voltage caused by the current. Number of electrode configurations were invented since the beginning of the last century, but only few has its common use (Wenner 1915, Schlumberger 1920, Al'pin 1950). These configurations are normally

used in two modes, profiling or sounding. In the sounding mode the separation between electrodes is progressively increased keeping centre of the array remains fixed at the same location. In profiling mode the relative positions of the electrodes are kept constant, while the entire electrodes array is moved along a profile for taking measurement at regular interval. In principle, sounding gives information about change in resistivity with depth, whereas profiling gives information about lateral change in resistivity.

Although geoelectrical sounding method is most suitable for the exploration of groundwater resources in the alluvium but it is still a challenging task to delineate saturated fractures in hard rocks due to its random distribution. If the geoelectrical sounding is conducted randomly then it may not coincide with the fractured zone and consequently fails to locate the presence of fractures at that point. For this reason, many geoelectrical soundings have to be conducted in the same area which may require relatively more time and associated costs. Karous and Mares (1988) established that the fractured zone has lower resistivity than the hard rocks and a good contrast exists between their resistivity.

Different types of gradient array along with their extensive geometries have been discussed in the literatures (Kunetz 1966, Bertin and Loeb 1976, Summer 1976, Kearey and Brooks 1984, Yadav 1988, Yadav et al 1997, Telford et al 1990). Theoretical response in terms of resistivity and chargeability over resistive and conductive veins present in the horizontal electric field has also been shown by Furness (1993, 1994). Further, Sharma (1997) discussed the role of gradient array with a mobile pair of potential electrodes for studying lateral variations in the resistivity of the ground. A generalized version of gradient profiling (GP) technique was recently tested to map the fractured zones and their inter connectivity for groundwater exploration by Yadav and Singh (2007, 2008).

The present paper deals a simplified layout of the gradient profiling technique. Accordingly, its geometrical factors have been computed and presented for its use by the interested users. Its application has been tested in the area of Rajiv Gandhi South Campus of Banaras Hindu University and its validation for detecting groundwater-saturated fractures has been attempted.

MATERIAL AND METHODS

A simplified version of the GP array in which a pair of current electrodes A and B was fixed at a distance of $AB=2S$ as shown in Figure 1. The central one-third space between the current electrodes $2S/3$ ($S/3$ both sides from centre O) can be scanned at regular intervals of 5m for the smallest possible spacing of potential electrodes i.e. $b=10\text{m}$ and 20m ($5b \ll S$) which satisfies the condition of gradient measurement.

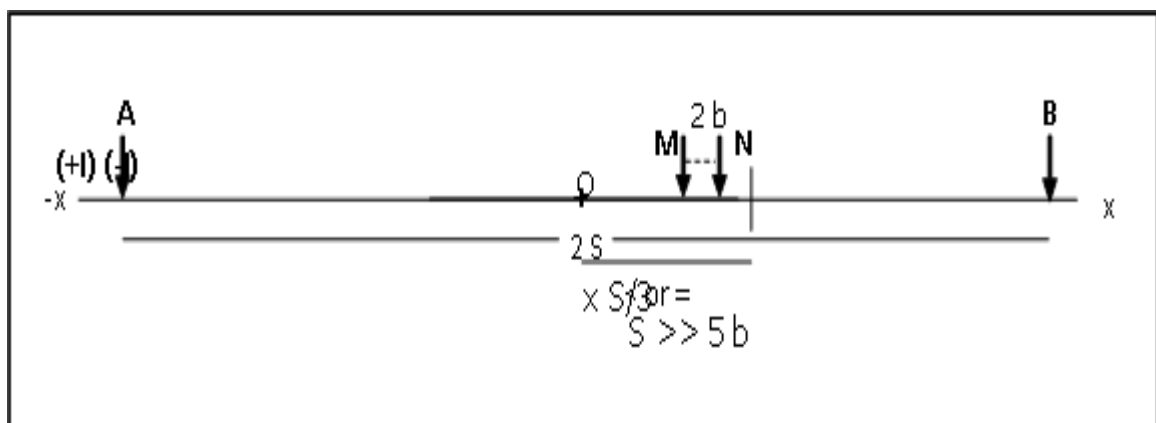


Figure 1: Layout of Gradient Profiling Array

The field apparent resistivity can be computed from the equation given as

$$\rho_a = G \frac{\Delta V}{I} \quad \dots \quad \dots \quad (1)$$

where $\frac{\Delta V}{I}$ = resistance between the measuring points, and G = geometrical factor defined as

$$G = \frac{2\pi}{\left(\frac{1}{(S+x-b)} - \frac{1}{(S-x+b)} - \frac{1}{(S+x+b)} + \frac{1}{(S-x-b)} \right)} \quad \dots \quad (2)$$

where S = the half-spacing between the current electrodes, b = the half-spacing between the potential electrodes, and x = the distance between the centers of the current and potential electrodes.

Using equation (2), the geometrical factor has been computed for three different values of $S=150\text{m}$, 300m and 450m and presented in Table 1. After taking one set of measurement, the entire array can be moved towards one side by a distance of either 100m , 200m or 300m depending upon the corresponding value of S to cover next segment of the profile in such a manner that the last measuring point overlaps the former one so that the new portion of the transect could be mapped and shift in the data of apparent resistivity can be rectified.

It can be further emphasized that the field strength and depth of penetration of current would be nearly constant in the central region bounded by $|x|=S/3$ in case of homogeneous earth. However, outside this region, under the similar earth condition, the depth of penetration of current would be decreased and accordingly horizontal electric field would be deviated due to influence of either current electrode A or B depending upon the case. These changes would produce response leading to false interpretation about the presence of inhomogeneities in real field condition. So, the configuration can be used to measure the horizontal electric field within the limit specified as $S/3 \geq |x| \geq 0$.

Hydrogeology of the Test Area

The study area lies between the latitudes $25^{\circ} 3' \text{N}$ to $25^{\circ} 4' \text{N}$ and longitudes $82^{\circ} 35.5' \text{E}$ to $82^{\circ} 36.5' \text{E}$ (Figure 2). The area is situated at high altitudes of about 170m - 150m from mean sea level (msl) which forms a plateau. The elevation of the surrounding area lies in the range of 110m – 90m from the msl. The Khajuri *Nadi* flows during monsoon season surrounding the plateau region in the south, east and north side follows low altitude and joins lower Khajuri reservoir. Although there is no major drainage system within the area under investigation but due to existing slope, i.e. NW–SE and then South ward, a small drainage is formed to flow the excess rain water of the plateau region during the rainy days (Figure 3). The plateau is covered by a very thin surface soil with varying thickness from place to place (1m – 2m) and few exposures of sandstone rocks (Krishnan 1982). The average annual rainfall is about 1090mm . The major source for recharging the area is rainfall during the monsoon season.

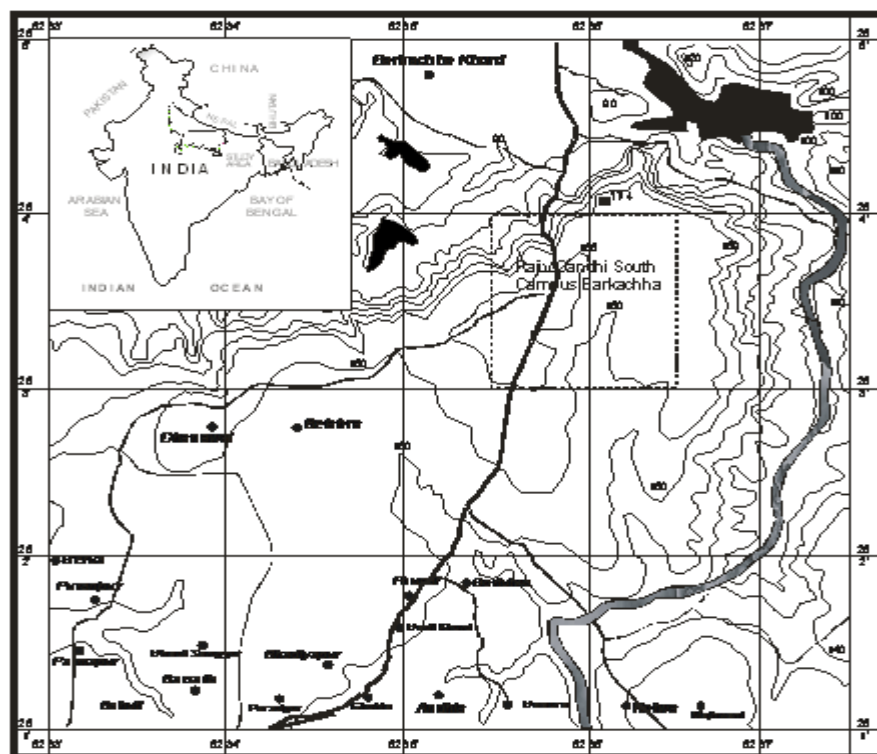


Figure 2: Location Map of the Study Area Along with Contours of Reference Level (MSL)

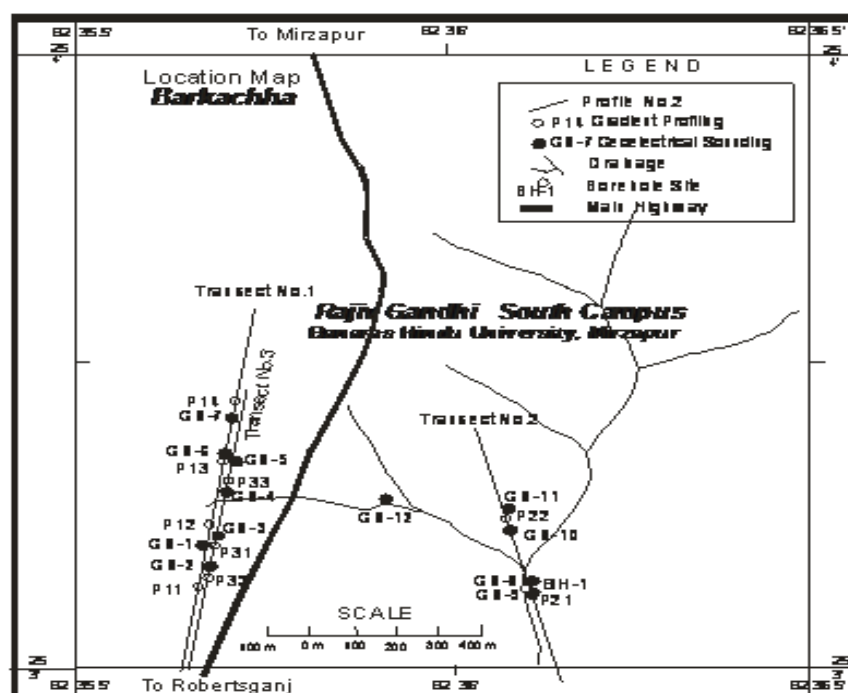


Figure 3: Map Showing the Location of Transects, Gradient Profiles (P_{11} , P_{12} ...) and Geoelectrical Sounding (GS), and Drilled Boreholes (BH)

The bedrock (Vindhyan Super Group of rocks) is expected below the surface soil cover since the area under study is lying in the close vicinity of the Vindhyan exposures (Krishnan 1982). The potential groundwater may occur in the weathered and fractured sandstone above the shale bed. These zones may be present even below the thin bed of semi-compact sandstone rocks. The amount of water that can be taken out from the fractured zone depends on size and

location of fractures, interconnection of the fractures and quantity of the material that may be clogging the fractures. It has often been observed that the minor fractures present in hard rocks, if interconnected with perennial source, give abundant groundwater. The geoelectrical surveys were conducted only at the selected locations, where ground surface was free from noise and suitable for laying out the array. Thus the entire area could not be mapped through the geoelectrical survey due to presence of high tension power lines and highly undulating ground surface. The locations of the resistivity survey conducted along transect (gradient profiling and geoelectrical sounding) are shown in figure 3.

RESULT AND DISCUSSIONS

Gradient Profiling

The gradient profiling (GP) were carried out along the three transects in the area with the help of a deep resistivity meter (DDR-4) along with a very sensitive potentiometer. The transect no. 1 was covered from the four setup of gradient profiles i.e. P₁₁, P₁₂, P₁₃ and P₁₄ using a fixed current electrode separation of 600m. The potential dipole separation was taken as 10m and 20m with an observation interval of 5m along a profile to cover 200m (100m both sides from the centre of the array) of length in the central region i.e. one-third of the profile. These two sets of data, for two separate separations of potential electrodes, were collected along the same profile only to check the reproducibility of readings during the measurement. Equation (1) was used to compute the field apparent resistivity for each gradient profile. The shifting in apparent resistivity observed at the overlap point was corrected with reference to its value obtained during previous profile. The linear scales have been used to plot the apparent resistivity and distance. The plotted apparent resistivity along this transect for both potential electrode spacing (MN values) closely follow similar trends (Figure 4). The analysis of the plotted curves clearly show that the apparent resistivity varies from medium to very high which indicates the rare possibility of presence for good fractures. Three locations were selected to conduct geoelectrical sounding out of the 'low' observed along this transect which are marked along the curve as GS-1, GS-6 and GS-7 in the Figure 4.

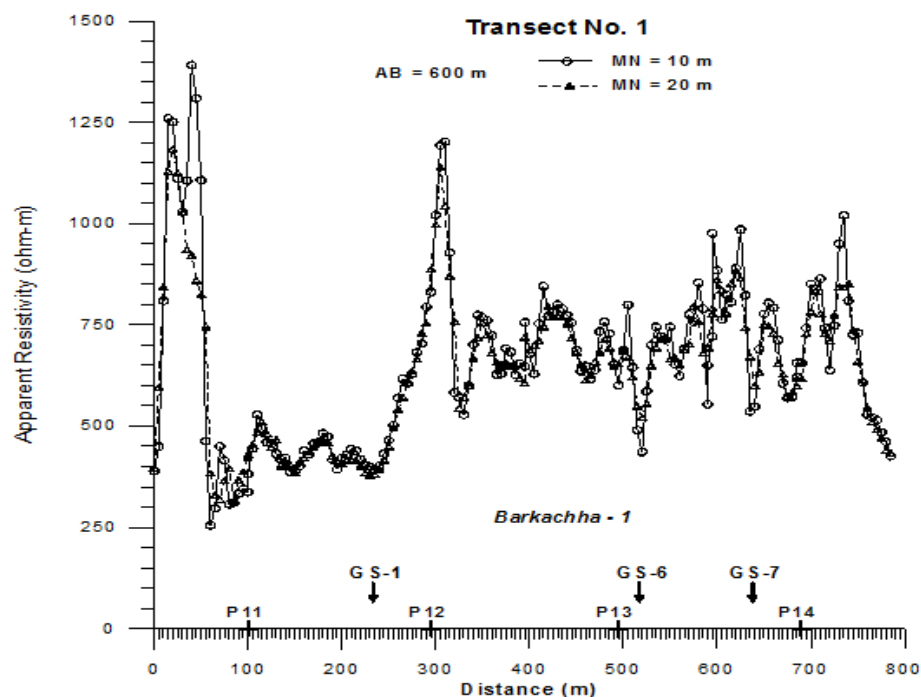


Figure 4: Responses of Gradient Profiling for Two Different Potential Electrode Separations (MN=10m and 20m) and for Fixed Current Electrode Separation (AB = 600m) along Transect-1

The transect no. 2 was carried out through two setup of gradient profiles i.e. P_{21} and P_{22} using a fixed current electrode separation of 600m. The same potential dipole separation of 10m and 20m was used with an observation interval of 5m along a profile to cover 200m of length in the central region i.e. one-third of the profile as done in the case of the previous transect. Equation (1) was again used to compute the field apparent resistivity. The correction for shifts at the overlap point was also applied. In this case also, the plotting of distance versus apparent resistivity data has been done on linear scales. The plotted apparent resistivity along this transect, for both spacing of potential electrodes (MN values), closely follows similar trends (Figure 5). The analysis of the plotted curve clearly shows that the apparent resistivity varies from moderate to high which indicates the modest possibility for the occurrence of good fractures. Based on the aforesaid criteria, four locations were selected along this transect also to conduct geoelectrical sounding, which are marked along the curve as GS-8, GS-9, GS-10 and GS-11 in the Figure 5.

Similarly, transect no. 3 was completed from the three setup of gradient profiles i.e. P_{31} , P_{32} and P_{33} , covering total length of 450m, using the same pattern of current electrode separation and potential dipole separation as done in the case of the previous transect. A total of 400m length was covered by the profiles P_{31} and P_{33} (200m each) and further 50m length was covered by the profile P_{32} towards one side only. Equation (1) was used to compute the field apparent resistivity and necessary corrections were applied as done for the earlier transect. The plotted apparent resistivity, for both potential electrode spacing (MN values) as shown in Figure 6, closely follows similar trends as observed along the previous transects. The analysis of the plotted curves clearly show that the apparent resistivity varies from medium to very high which indicates the lesser degree of fracturing with limited extent. In the similar pattern, four locations were also selected to conduct geoelectrical sounding along this transect which are marked along the curve as GS-2, GS-3, GS-4 and GS-5 in the Figure 6.

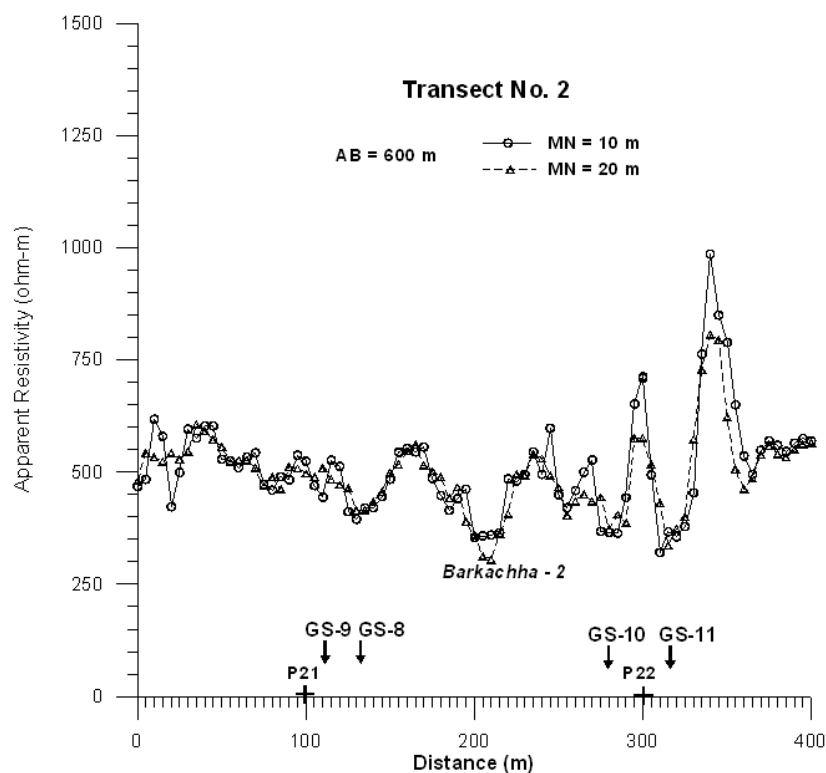


Figure 5: Responses of Gradient Profiling for Two Different Potential Electrode Separations (MN=10m and 20m) and for Fixed Current Electrode Separation (AB=600m) along Transect-2

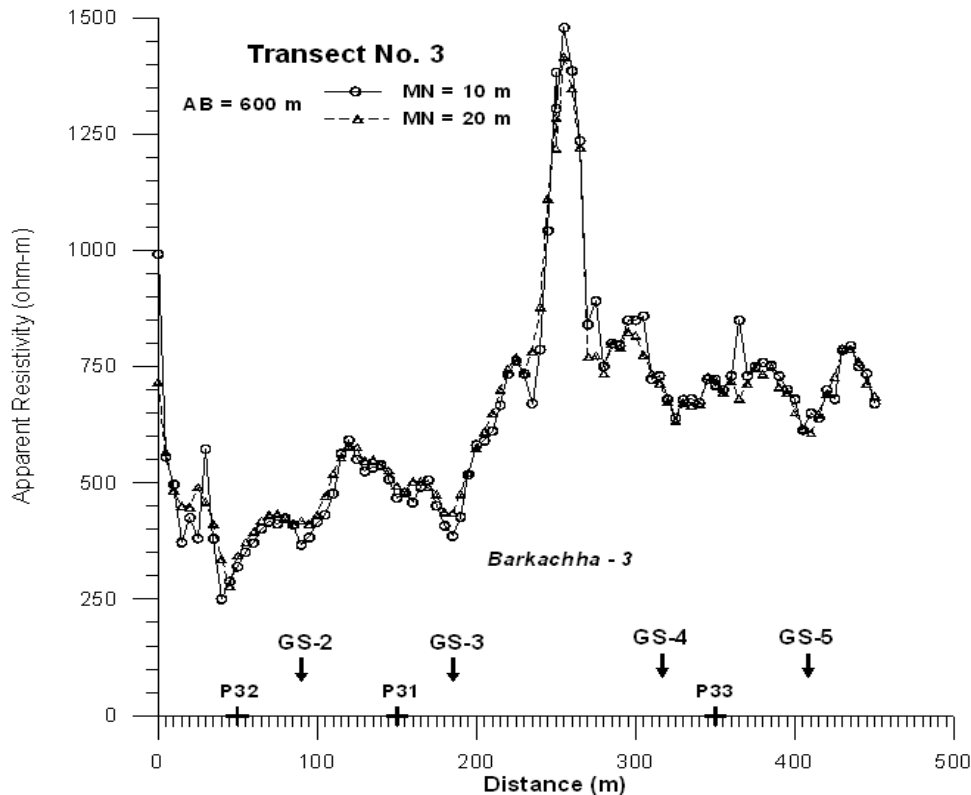


Figure 6: Responses of Gradient Profiling for Two Different Potential Electrode Separations (MN=10m and 20m) and for Fixed Current Electrode Separation (AB=600m) Along Transect-3

The prominent low observed along the transect-1 having lowest apparent resistivity of the order of 250ohm-m, at a distance of 40m towards the south side from the centre of the profile P₁₁, was observed as shown in Figure 4. Figure 5 shows the variation of apparent resistivity along transect-2, far away about 600m towards the east from the transect-1 using similar setup. The variation of apparent resistivity along this profile is comparable to the previous one. The prominent low on this transect has lowest value of apparent resistivity as 300ohm-m in the middle of the profiles P₂₁ and P₂₂. Similarly, Figure 6 shows the response obtained along transect-3 which was taken close to transect-1. The prominent low observed along this transect has a similar characteristic which indicates the presence of similar nature of fractures with varying degree of fracturing. The above study clearly indicates the presence of fractures within the hard rocks but of limited extent. The higher range of 'low' apparent resistivity suggests that these fractures are associated with low degree of fracturing resulting into low porosity and permeability.

Geoelectrical Sounding

For the quantitative evaluation of the fractures few geoelectrical soundings were conducted at selected locations – based on the 'low' observed from the gradient profiling along the transects which are marked (Figures 4, 5 and 6). Accordingly the geoelectrical soundings were carried out at these locations using Schlumberger configuration as shown in the location map (Figure 3). The geoelectrical sounding was aligned along gradient profiling transect as the required space for laying out the array was available there only. The measurement of apparent resistivity was made for different AB/2 spacing (i.e. half of the distance AB) as per the requirements for the Schlumberger sounding. The successive AB/2 separation was taken as approximately 1.25 times the previous separation so that they are linearly distributed between 2.5m and 300m in the logarithmic scale. The layer parameters were initially obtained using a partial curve matching technique

(Keller and Frischknecht 1966, Bhattacharya and Patra 1968, Koefoed 1979) with the help of three layer master curves (Rijkswaterstaat 1969) and auxiliary point charts (Ebert 1943). These parameters were used as initial model input for the computer assisted interpretation program named as 'Automatic Iterative Method of Resistivity Sounding Interpretation' (AIMRESI) developed by the author (Yadav 1995) based on the steepest descent technique of the Newton-Raphson iterative method. The AIMRESI program needs field data and initial model parameters, which finally gives an improved model along with the associated r.m.s. error of less than 1% – 2% for a fixed number of iterations. These layer parameters were also corroborated with the results obtained from 1X1D V3.2 software of Interpex Ltd. Thus the interpretation of the geoelectrical sounding curve is accomplished in terms of the layer parameters for all the locations which are presented in table 2. Based on the resistivity and thickness of the layer, some locations show the presence of fractures of limited extent which can be utilized for the exploitation of groundwater resources.

A test borehole was drilled near GS-8 location. The layer parameters derived from the sounding data show good correlation with the borehole lithologs as shown in Figure 7. The lithological units have been identified based on the resistivity value and the drilling data. A fracture zone of 11m thick was present at a depth of 43m and was continued up to the depth of 54m. However, thickness obtained through sounding results was 9m which is within the acceptable limit. The resistivity of the fractured zone was obtained as 232ohm-m. After this, semi-compact sandstone was encountered. The drilling was stopped at a depth of about 119m because the same formation continued even up to this depth. The groundwater discharge was obtained as 8,000 liters per hour (lph) which is not sufficient to fulfill the demand of water supply for the Rajiv Gandhi South Campus of Banaras Hindu University.

The study reveals that the fractures are randomly distributed in the area. The degree of fracturing is neither enough to restore sufficient amount of water nor interconnected with any perennial source of groundwater from the surrounding region as the entire area is situated at a high altitude compared with the neighboring ground level. The qualitative interpretation of gradient profiling data clearly indicates that the technique is quite effective in the hard rock area and it did indicate the presence of fractures within the hard rocks, thereby assisting in groundwater investigations. The interpretations presented above clearly indicate that the geoelectrical soundings taken over the fractured zones (identified from GP survey) are quite successful. It is to be emphasized that the 'lows' having smaller magnitude obtained along the gradient profiles may not indicate the presence of good fractures having good potential of groundwater. Such 'lows' may be due to either less fracturing or fractures not fully saturated with groundwater. It can be inferred from the present study that potential groundwater may be found when the apparent resistivity observed in the range of 150 ohm-m – 500ohm-m for that 'low' anomaly through GP survey.

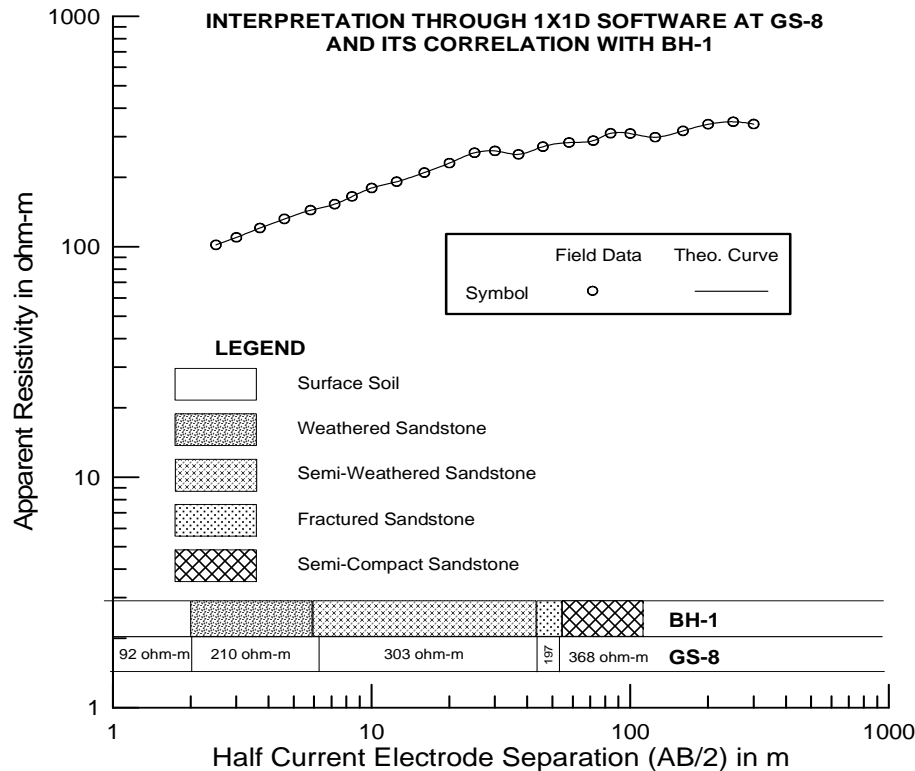


Figure 7: Correlation of the Results of Geoelectrical Layer Parameters (Thickness & Resistivity) Obtained from Geoelectrical Sounding GS-8 and Lithologs of a Borehole BH-1 Drilled Close to GS-8 Location

CONCLUSIONS

The efficiency of GP survey is proved for delineation of the weathered and fractured zones in hard rock areas. The GP survey is very helpful in distinguishing the prospective sites to delineate hydrogeological features and to avoid unsuccessful attempts of conducting sounding at several randomly selected locations – which significantly minimizes the cost and time of geoelectrical surveys. The present study suggests that the simplified version of gradient profiling technique for groundwater exploration, especially in hard rock areas, can be advantageously applied not only in India but also in other countries.

ACKNOWLEDGEMENTS

Author is grateful to the Department of Geophysics, Banaras Hindu University for providing the necessary facilities required for the geoelectrical survey. Technical support provided by Departmental Research Scholar namely Mr. S.K. Singh during survey are duly acknowledged. Thanks are also due to Prof. T. Lal and Prof. K.M. Srivastava, Department of Geophysics, Banaras Hindu University for critically going through the manuscript and for giving valuable suggestions.

REFERENCES

1. Al'pin, L. M. 1950. *The theory of dipole sounding; Gostoptekhizdat, Moscow.* (Trans. In: *Dipole methods for measuring conductivity, Plenum Press, New York 1966*).
2. Bertin, J. and Loeb, J. 1976. *Experimental and theoretical aspects of IP. Vol. 1. Presentation and application of the IP method – Case histories. Gebruder Borntraeger, Berlin, 250 p.*

3. Bhattacharya, P. K. and Patra, H. P. 1968. *Direct current geoelectric sounding*. Elsevier, Amstardam.
4. Ebert, A. 1943. *Grundlagen zur Auswertung geoelektrischer Tiefenmessungen (Basics in interpretation of geoelectrical depth measurements)* *Gerlands Beiträge zur Geophysik*, **10(1)** 1-17.
5. Furness, P. 1993. *Gradient array profiles over thin resistive veins* *Geophysical Prospecting* **41** 113-30.
6. Furness, P. 1994. *Gradient array profiles over conductive veins* *Exploration Geophysics* **25** 61-70.
7. Karous, M. and Mares, S. 1988. *Geophysical methods in studying fracture aquifers* *Charles University, Prague [ER, EMI, SP, SRR, borehole]*.
8. Kearey, P. and Brooks, M. 1984. *An introduction to geophysical exploration* *Blackwell Scientific Publications, Oxford, London*, 296 p.
9. Keller, G. V. and Frischknecht, F. C. 1966. *Electrical methods in geophysical prospecting* *Pergamon Press, New York*.
10. Koefoed, O. 1979. *Geosounding principles (1. Resistivity sounding measurements, methods in geochemistry and geophysics)*. Elsevier, Amsterdam, Oxford, New York.
11. Krishnan, M. S. 1982. *Geology of India and Burma (6th Edition)* *CBS publishers and distributors, New Delhi*
12. Kuntz, G. 1966. *Principles of direct current resistivity prospecting* *Gebrüder Borntraeger, Berlin*, 250 p.
13. Rijkswaterstaat. 1969. *Standard Graphs for Resistivity Prospecting*. EAEG, The Netherlands.
14. Schlumberger, C. 1920. *Etude sur la prospection électrique du sous-sol*. Gauthier: Villars, Paris.
15. Sharma, P. V. 1997. *Environmental and Engineering Geophysics* *Cambridge University Press, New York*, 475 p.
16. Summer, J. S. 1976. *Principles of IP for geophysical exploration* *Elsevier, New York*
17. Telford, W. M., Geldart, L.P. and Sheriff, R. E. 1990. *Applied Geophysics (II Ed.)* *Cambridge University Press, U.K.*, 790 p.
18. Wenner, F. 1915. *A method of measuring earth resistivity* *U.S. Bur. Standards, Science Paper*, **258**, 469-78.
19. Yadav, G. S. 1988. *Pole-dipole resistivity sounding techniques for shallow investigation in hard rock areas* *Pure & Applied Geophysics* **127(1)** 63-71.
20. Yadav, G. S. 1995. *A FORTRAN computer program for the automatic iterative method of resistivity sounding interpretation* *Acta. Geod. Geoph. Hung.* **30 (2-4)** 363-77.
21. Yadav, G. S. and Singh, S. K. 2007. *Integrated resistivity surveys for delineation of fractures for groundwater exploration in hard rock areas* *Journal of Applied Geophysics* **62** 301-12.
22. Yadav, G. S. and Singh, S. K. 2008. *Gradient profiling for the investigation of groundwater saturated fractures in hard rocks of Uttar Pradesh, India* *Hydrogeology Journal* **16** 363-72.

APPENDICES

Table 1: Geometrical Factors for Gradient Profiling for Different Current and Potential Electrode Spacing

(a): Current Electrode Spacing AB=300 m or Half-Current Electrode Spacing $S = 150$ m			(b): Current Electrode Spacing AB=600 m or Half-Current Electrode Spacing $S = 300$ m			(c): Current Electrode Spacing AB=900 m or Half-Current Electrode Spacing $S = 450$ m		
x (m)	$b = 10$ m	$b = 20$ m	x (m)	$b = 10$ m	$b = 20$ m	x (m)	$b = 10$ m	$b = 20$ m
0	3520	1736	0	14127	7040	0	31806	15879
5	3508	1730	5	14115	7034	5	31794	15873
10	3473	1712	10	14080	7016	10	31759	15856
15	3415	1683	15	14021	6987	15	31700	15826
20	3335	1642	20	13939	6946	20	31618	15785
25	3234	1591	25	13835	6893	25	31512	15732
30	3115	1530	30	13708	6829	30	31384	15668
35	2979	1461	35	13559	6755	35	31232	15592
40	2829	1385	40	13389	6669	40	31059	15505
45	2666	1302	45	13199	6574	45	30863	15407
50	2493	1214	50	12989	6469	50	30646	15298
			55	12761	6354	55	30407	15178
			60	12515	6230	60	30147	15048
			65	12252	6098	65	29867	14908
			70	11973	5958	70	29567	14758
			75	11680	5811	75	29248	14598
			80	11373	5657	80	28910	14429
			85	11054	5497	85	28554	14250
			90	10724	5331	90	28181	14063
			95	10384	5161	95	27791	13868
			100	10036	4986	100	27384	13664
						105	26963	13453
						110	26527	13235
						115	26077	13010
						120	25614	12778
						125	25139	12540
						130	24652	12296
						135	24155	12047
						140	23648	11793
						145	23132	11534
						150	22607	11272

Table 2: Geoelectrical Layer Parameters

Layer No./ GS No.	Layer-1		Layer-2		Layer-3		Layer-4		Layer-5		Layer-6
	Resistivity (ohm-m)	Thickness (m)	Resistivity (ohm-m)	Thickness (m)	Resistivity (ohm-m)	Thickness (m)	Resistivity (ohm-m)	Thickness (m)	Resistivity (ohm-m)	Thickness (m)	
1	21.7	2.7	494	1.0	7232	5.0	152				
2	31.7	2.3	2943	1.9	64	5.9	179	22.4	32	39.9	4192
3	5.4	1.1	4775	5.8	102						
4	57.9	2.1	857	31.6	130	26.6	2542				
5	35.3	1.8	2353	0.1	504	114.8	213				
6	62.8	1.1	2.6	0.3	510	45.6	218				
7	11.3	1.0	1130	1.2	60	3.1	1537	4.9	275		
8	92.3	2.0	210	4.2	303	38.1	232	9.0	369		
9	53.6	1.0	243	10.5	980	7.9	131	10.8	445		
10	317.1	2.1	1929	1.8	306	55.5	96	31.6	486		
11	127.2	1.0	8644	1.8	232	2.7	175	2.0	149	7.2	385
12	310.0	2.0	25792	1.0	319	1.9	2353	7.0	96.5	18.1	466

